"IDEAL" TWO DIMENSIONAL GRAIN GROWTH

James A. Glazier
AT&T Bell Laboratories
600 Mountain Avenue
Murray Hill, NJ 07974

Gary S. Grest and Michael P. Anderson
Corporate Research Science Laboratory
Exxon Research and Engineering Company
Annandale, NJ 08801

Abstract

We discuss the nature of "ideal" two dimensional grain growth and deviations from it in real experiments and models, concentrating on the soap froth and Potts model.

Simulation and Theory of Evolving Microstructures
Edited by M.P. Anderson and A.D. Rollett
The Minerals, Metals & Materials Society, 1990

Introduction

While grain growth in time is an extremely common natural process, even in the simplest case of two dimensional coarsening the characterization of "ideal" grain growth is still incomplete (1 ,2). In experiments we must use real rather than ideal materials and we must try to separate the underlying "universal" behavior from effects due to the material's particular properties. In theoretical treatments we must make approximations since no exact analytical solutions for grain growth exist. In this paper we discuss "ideal" grain growth, making a detailed comparison between experimental observations of a two dimensional soap froth (which is usually taken as the closest experimental approximation to ideal growth) and the predictions of the two dimensional large Q Potts model (3).

Experimental and Model Systems

There are many experimental systems which exhibit grain growth or coarsening in time, including metallic and ceramic recrystallization, magnetic materials, lipid monolayers, biological aggregates and soap froths. There are a similar variety of models for coarsening including simple mean field theories which look only at distributions (4, 5), mean field theories which include topology (6, 7), "exact" models which calculate the motions of boundaries or vertices (8, 9, 10, 11, 12), and the Potts model which takes a microscopic approach to modeling (13, 14, 15, 16). In all such systems, surface energy driven diffusion leads to the motion of curved boundary walls causing certain grains to grow while others shrink and disappear. Whenever a grain disappears its neighbors gain or lose sides and change their rates of growth. The result is a gradual increase in the overall length scale of the grains. This basic dynamics interacts with the geometrical constraint that vertices are three-fold connected to produce a family of typical patterns of coordination number three. Typically, coarsening in the soap froth begins with a nearly regular array of hexagonal grains and gradually evolves into a completely disordered pattern with time invariant distributions of number of sides per grain and grain areas (a **scaling state**). In metals and the Potts model the typical initial condition is a completely random distribution which segregates to form domains.

In a soap froth experiment we fill a cell (typically 8.5 x 11.5 x 1/8 inches) with a well ordered array of small bubbles (typically 10,000 bubbles) (17). The excess fluid in the films accumulates on the top and bottom plates of the cell in **Plateau Borders**, which are much broader than the films themselves. These borders may change the evolution of the froth (there is no reason to suppose that they have a linear bending energy for example) but they do allow us easily to record the pattern by placing it level on a photocopier, and photocopying periodically. Photocopying heats the froth and can occasionally cause walls to break. The total number of walls broken during a run is less than .1% of the total side redistribution, but nevertheless results in a slightly greater number of very many-sided bubbles. The only real control parameters are the temperature, type and pressure of the gas and the total volume of fluid in the Plateau borders. The detailed properties of the fluid are not important as long as its viscosity is small .

Vertex and boundary dynamic models arise naturally from a consideration of the basic physics of a soap froth, in which gas diffuses across well defined soap films. The Potts model puts surface tension on a lattice by defining an energy which is proportional to the total length of grain boundary in the system. We define on each site of our lattice, a spin $\sigma(i,j)$, where all the lattice points lying within a given grain in our initial configuration are assigned the same value of spin, with a different spin for each grain. Since we denote the number of different degenerate spins in the model by Q, we have a $Q=$ number-of-grains Potts model. However, since each grain is separately labelled, we generally refer to it as the

$Q=\infty$ case. The energy of interaction between like spins is defined to be zero, and between unlike spins to be one. Thus the total Hamiltonian is:

$$H = -\sum_{i',j'} \sum_{neighbors\ i',\ j'} \delta_{\sigma(i,j),\sigma(i',j')} - 1, \qquad (1)$$

where the range of the second sum affects the nature of the interaction. The spins are flipped using a Monte-Carlo selection, where a spin is chosen at random and flipped only if the flip would lower system energy. This method of selection corresponds to the zero temperature limit. The temperature remains a useful control parameter, however, for the analysis of conditions where fluctuations are significant. With sufficient coarse graining the result is an effective surface tension, albeit an anisotropic one. Note that, unlike the soap froth, the Potts model is not deterministic.

Ideal Grain Growth

What do we mean by ideal grain growth? At one level this is a straightforward question, provided that we recognize that the terminology used to describe the coarsening of a froth and recrystallization in a metal is slightly different. The basic mechanism in grain growth is the interaction of topological constraints with energy minimization. The quantity to be minimized is the total film (grain boundary) length, the constraint that films cannot break, so that individual grains are well defined objects. We assume that the rate of change in size of grains is slow so that the pattern is in mechanical equilibrium at all times. Energy minimization and mechanical equilibrium imply that: 1) all vertices are threefold and all vertex angles are 120° and 2) all walls are sections of circular arcs (in three dimensions all angles must be tetrahedral and all walls spherical caps). At equilibrium, pressure (surface energy) is constant throughout a grain so 3) the pressure difference across a wall, ΔP, is proportional to the reciprocal of the radius of curvature and thus 4) the rate of gas (atomic) diffusion across a wall is proportional to the product of the wall's length with the pressure difference. We assume incompressibility so that 5) mass and area diffusion are equivalent. These hypotheses immediately imply an exact result, von Neumann's law for the rate of change in area of an n-sided grain (18):

$$\frac{da_n}{dt} = \kappa(n-6), \qquad (2)$$

where κ is an effective diffusion constant with units of area/time. This relation has been checked experimentally in the soap froth (see Fig. 1) and found to hold on average to within experimental error (17, 19, 20). It is also obeyed statistically in Potts model simulations (15). Already we encounter a difficulty. von Neumann's law is exact, i.e. it predicts the rate of growth for each individual bubble, yet in both experiment and model it is obeyed only by ensembles, not by individuals (19, 20). We also find that in neither the froth nor the Potts model is the 120° rule strictly observed (22). In the soap froth we find that the typical bubble is more polygonal than it should be (see Fig. 2). Interestingly, the angle deviations are such that a modified version of von Neumann's law which includes angle deviations yields a result almost indistinguishable from the unmodified version (20). In the Potts model the vertex angles assume discreet values which depend on the lattice

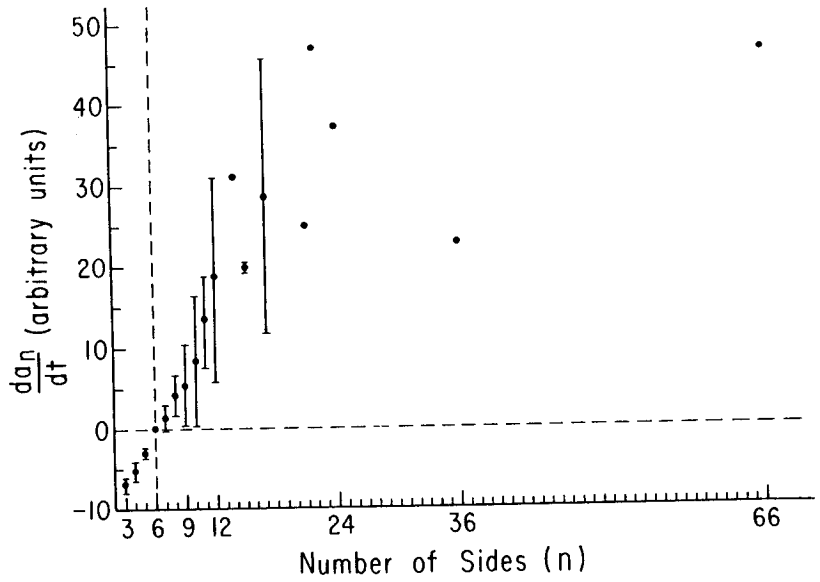

Figure 1 -- von Neumann's Law. Experimental measurement of growth rate versus number of sides in a soap froth (from ref. 20).

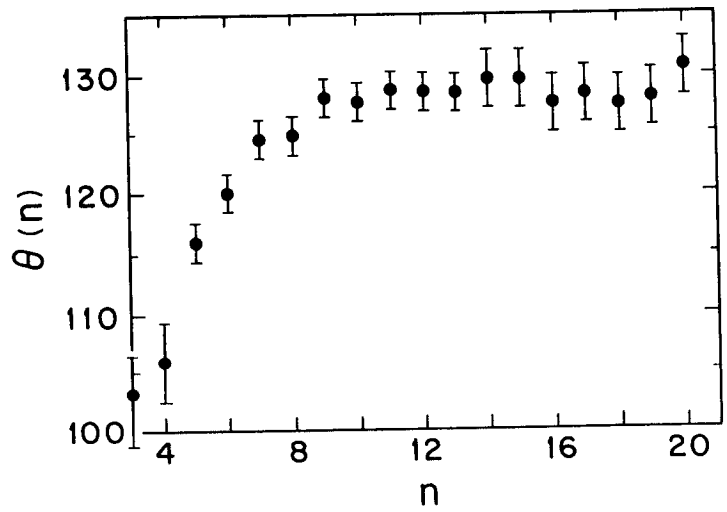

Figure 2 -- Angle Deviations. Average internal angle of an n-sided bubble versus n (from ref. 22). Note that walls are sections of circular arcs.

structure and cannot be 120° on a square lattice. In both cases these angle fluctuations may partially account for fluctuations in the growth rates of individual grains. The Potts model and most real metals also violate rule 2) because the rate of diffusion across and along grain boundaries is the same allowing boundary profiles far from equilibrium shapes.

von Neumann's law has one immediate consequence for the overall dynamics of pattern evolution. In a scaling state the average area per grain, <a>, in the whole pattern must grow linearly in time (4, 17, 20). Such behavior is difficult to observe both experimentally where the exponent α describing the rate of area growth,

$$\langle a \rangle \propto t^{\alpha}, \tag{3}$$

is almost always less than one (typically 0.59 ± 0.11 for the soap froth and between 0.1 and 0.9 for metals) (2, 17, 19), and in microscopic models like the Potts model where the time to reach the scaling state is very long (13). In soap froths the anomalous exponent is associated with a gradual decrease of the effective diffusion constant, resulting from the broadening of the Plateau borders as the total length of soap film decreases with time (which reduces the height of film available for diffusion) and possibly also from thickening of the films themselves (21). In metals, impurity segregation can reduce grain boundary mobility, as can differential etching effects in thin films (2). In the Potts model, strongly anisotropic lattices can support vertex angles deviating from 120° and hence reduce the curvature of grain boundaries, which gradually align along energetically preferred directions. Flatter boundaries cause slower diffusion so coarsening slows and may even stop, again yielding growth exponents less than one (13) (the same effect is observed in strongly anisotropic metals at low temperatures). Larger exponents are obtained at higher temperatures where fluctuations overcome anisotropy pinning (3, 13). However, the soap froth is essentially fluctuation free, and therefore should be simulated in the zero temperature limit. A better solution is to use a nearest neighbor hexagonal lattice (energy ratio 1.15) or a next nearest neighbor square lattice (energy ratio 1.13), to reduce pinning. There is still some preferred boundary alignment in both cases (e.g. along 45° and 90° orientations in the square lattice as seen in Fig. 3), but $\alpha = 1$ and there is no evidence of freezing up to the length scale of the simulation (15).

If von Neumann's law were all there were to froth evolution the problem would be trivial; however, when grains disappear their neighbors gain or lose sides, resulting in continual changes in each grain's rate of growth or shrinkage. There are two basic processes at work here: the **T1** process, in which two bubbles come to share (and gain) a side, pushing apart two previously neighboring bubbles which lose a side (side swapping), and the **T2(3)** process, in which a three-sided bubble disappears, each of its neighbors losing a side. While the $T2$ process is straightforward to treat theoretically it is extremely difficult to predict $T1$'s without using an exact geometrical model. Furthermore, in real materials, four- and five- sided bubbles can also disappear directly, resulting in more complicated patterns of side redistribution which are certainly deterministic but essentially unpredictable (in fact side redistribution can be shown to be a chaotic process) (2). In general, given a picture of a bubble about to disappear we do not know how to predict the changes in number of sides of its neighbors. The difficulty in most models is to treat the redistribution of sides correctly, whether we put in assumptions concerning redistribution correlations (as in mean field theories) or whether it is taken care of automatically, either deterministically as in vertex and boundary models, or probabilistically as in the Potts model. We do not even know if the soap froth in the presence of Plateau borders really has the same correlations as an "ideal" system. The boundary model of Frost and Thompson ought to be close to "ideal"

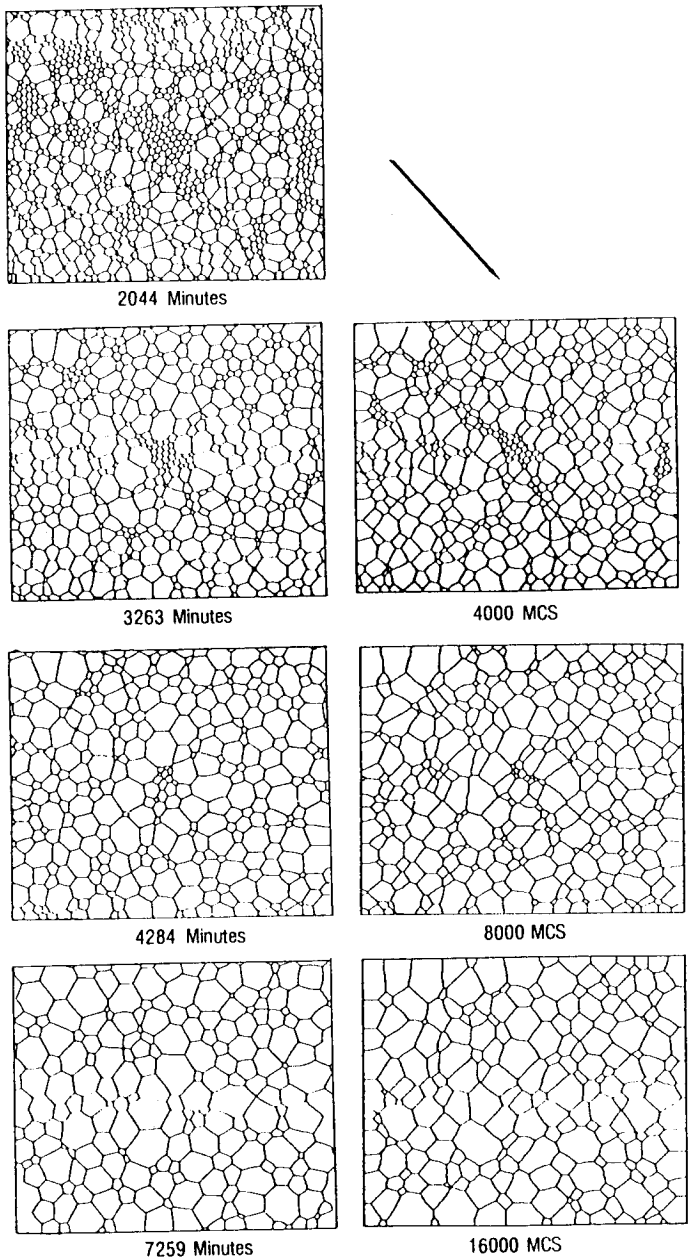

Figure 3 -- Evolution of soap froth (left) and the square lattice Potts model (right) using the state of the soap froth at t=2044 minutes as the initial condition (right).

but the correlations it predicts have never been analyzed (8, 11).

In the $Q=\infty$ Potts model neither the motion of domain boundaries nor the disappearance of domains can lead to contact and hence coalescence of separate domains with the same spin type. Hence we explicitly exclude wall breakage from the simulation. Finite Q Potts models allow grain coalescence and correspond to nonzero rates of wall breakage. In both cases, coalescence is a random process different from diffusive coarsening.

The effect of side redistribution is seen most clearly in the disordering of a nearly perfect hexagonal lattice of soap bubbles (17). Since six-sided bubbles do not evolve the initial rate of area increase is very slow. As few-sided bubbles in the grain boundaries disappear, their neighbors gain or lose sides and begin to grow or shrink themselves. Thus disorder eats away at hexagonal domains. The rate of evolution increases to a maximum during which the presence of residual small six-sided bubbles results in broad area and number of side distributions. Finally, when all of the initial order and length scale disappears, the distributions narrow to a scaling state and the rate of growth slows to a power law.

Comparison Between Theory and Experiment

We use two different types of Potts models for our simulations: a second nearest neighbor interaction on a square lattice compatible with our image digitization to allow direct comparison to experiment, and a nearest neighbor interaction on the triangular lattice to gather statistics on the equilibrium state (3). The simulations on the triangular lattice ran with $Q = 48$, starting from a random initial state on a 1000 x 1000 lattice with periodic boundary conditions. The simulations on the square lattice square lattice ran on a 600 x 500 square lattice with $Q = \infty$ and open boundary conditions (in which spins on the boundary were assumed to interact with frozen imputities). To compare the results of the two simulations we renormalize the time in the square lattice simulations by $48/Q_{max}$, where Q_{max} is the initial number of grains.

We ran the square lattice Potts model simulation using two different initial conditions, employing digitized soap froth images at $t = 0$ minutes (2490 grains) and $t = 2044$ minutes (1175 grains) as the starting patterns. The $t = 0$ minutes initial pattern was composed almost entirely of hexagonal bubbles of nearly equal area while the t=2044 minutes pattern had evolved sufficiently that there are were few islands of six-sided bubbles remaining from the initial fill.

The qualitative features of the disordering were similar for the two simulations and the experiment (we compare the experiment and the t=2044 minutes simulation in Fig. 3), though the differing boundary conditions (the sample of the froth was taken from the bulk whereas the simulation had open boundary conditions) resulted in a rapid divergence between the actual patterns. In the simulation starting from the $t = 2044$ minutes soap froth image the disappearance of residual order occurred in both systems at comparable length scales (after an increase of approximately one order of magnitude), and the qualitative patterns remained comparable (We use the conversion that time is the number of MC steps times 0.32, $t=t_{mc}*0.32$). Regardless of the initial random seed, the simulation starting from the $t = 0$ minutes soap froth image retained its hexagonal pattern for much longer than the froth. Apparently six-sided bubbles are less likely to change their number of sides in the simulation than in a real froth. Once the blocks of hexagons disappeared, however, and the length scale grew, the rates of evolution of the two simulations and the experiment were similar and the long term states of the $t = 0$ and $t = 2044$ minutes square lattice Potts model simulations were indistinguishable. The difference in initial rate of growth indicates a fundamental though subtle difference in side redistribution between the simulation and

real froth. However, it is difficult to say whether it is a true effect of an increased stability of hexagonal bubbles in the Potts model or, as suggested by the good agreement at larger length scales, results from the length scale of the initial condition in the simulation being small compared to the lattice constant.

In Fig. 4 we compare the average bubble size versus time for the froth and square lattice Potts model simulations. We found essentially exact agreement between the froth and the t = 2044 minutes simulation up to 20,000 minutes where the statistics are best, after which both showed fluctuations. The initial rate of area growth of the t = 0 minutes simulation was significantly slower than the froth, suggesting that the Potts model had more difficulty in converting order to disorder. In both cases the typical qualitative dynamics for coarsening of an initially ordered froth appeared: slow initial evolution, followed by rapid growth during which any residual order disappeared, and a long term tail with slower power law growth (17). The growth exponent of both simulations was slightly higher than in the froth, but all were consistent with linear growth in time, i.e. $\alpha = 1$.

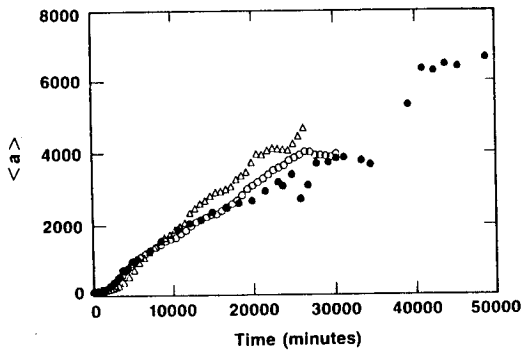

Figure 4 -- Average bubble area versus time for soap froth (bullets), square lattice Potts model simulation starting from the digitized soap froth image at t = 2044 minutes (open circles), and square lattice Pottts model simulation starting from the digitized soap froth image at t = 0 minutes (triangles).

Distribution Functions

Besides the mean bubble area, the two basic measures of the state of a froth are the distribution of the number of sides ($\rho(n)$, the probability a randomly selected bubble has n sides) and the normalized area distribution ($\rho(a/\langle a\rangle)$, the probability that a bubble has an area which is a given fraction of the mean bubble area). We define the mth moment of the side distribution as:

$$\mu_m = \sum_{n=2,\,\infty} \rho(n)(n-\langle n\rangle)^m, \qquad (4)$$

where $\langle n\rangle$ is the average number of sides of a bubble in the pattern (for infinite patterns $\langle n\rangle$=6). We sum from n=2 because two-sided grains can occur in metallic and other materials. Moments higher than μ_2 are sensitive to the large n tail of the distribution, which is subject to counting error.

At approximately 10,000 minutes (see Fig. 4), just after the rate of evolution rolls over to a power law, the distribution becomes essentially time independent, confirming the existence of the scaling state noted by Stavans and Glazier (3, 22). We plot the scaling distribution for the triangular lattice Potts model simulation and for the froth in Fig. 5(a). While $\rho(n)$ for the simulation lies within the range of experimentally measured values for each n, the froth has fewer four-and many-sided bubbles. Interestingly, the Q = 48 triangular lattice Potts model with wall breakage gives nearly identical distributions to the $Q = \infty$ square lattice Potts model without. We are currently studying in detail the effect of lattice geometry and anisotropy on Potts model grain growth.

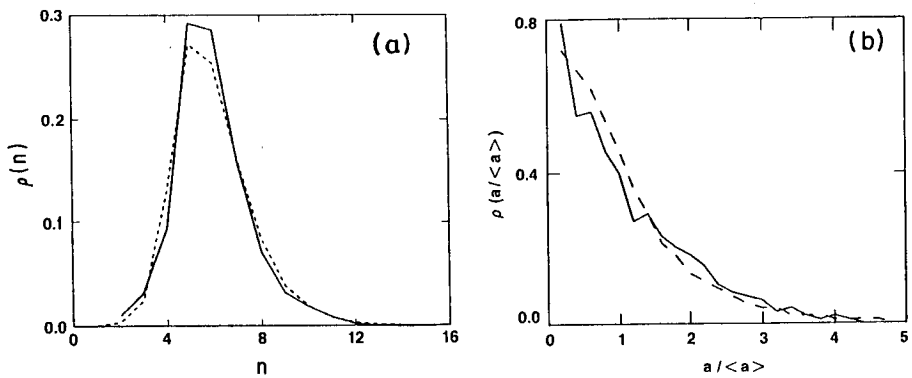

Figure 5 -- (a) Side distribution in the scaling state for soap froth (solid) and triangular lattice Potts model (dashed). (b) Fractional area distribution in the scaling state for soap froth (solid) and triangular lattice Potts model (dashed).

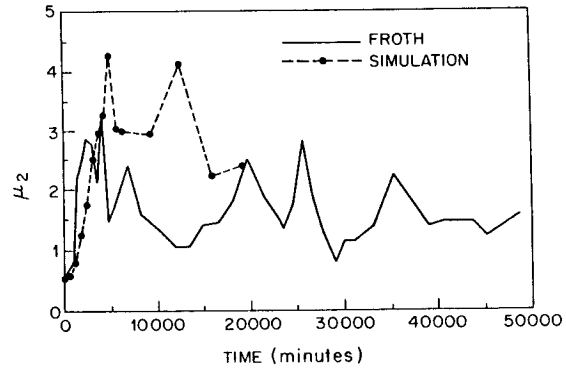

Figure 6 -- Second moment of the side distributions versus time for the soap froth (solid) and square lattice Potts model starting with the t=0 minutes digitized soap froth image (dashed).

Looking at the time evolution of the moments in the experiment (Fig. 6), we find an initial value of $\mu_2 = 0$, which widens to a maximum width $\mu_2 = 3.25$, then narrows to a stable value of $\mu_2 = 1.5 \pm 0.3$, in agreement with the value $\mu_2 = 1.5 \pm 0.2$ measured by Stavans and Glazier. In the simulation, μ_2 is qualitatively the same, but increases slightly more slowly at short times and peaks slightly later and at a higher value of $\mu_2 = 4.4$. It then

decreases to an equilibrium value of 2.4 ± 0.1. The third moment, which measures the strength of the large n tail, begins near zero, increases rapidly to a maximum during equilibration when the frequency of many-sided bubbles is maximal ($\mu_3 = 4.5$), then drops to a stable value of $\mu_3=1.0 \pm 0.5$. The simulation reaches a maximum value of $\mu_3=16.6$ and drops to an equilibrium value of $\mu_3=5.25 \pm 1.25$. The model also gives larger values than the froth for the forth moment but agrees well with Fradkov, Shvindlerman and Udler's measurement of two dimensional grain growth in Al $+10^{-4}$ Mg foil (23).

The agreement between the low moments and the disagreement for the higher moments implies that the simulations create a few more very many-sided bubbles than the real froth. These extra bubbles suggest that side shedding is more strongly anticorrelated in the froth than in the simulations.

In spite of the large error bars on our distribution measurement, the scaling state side distribution of the soap froth is surprisingly difficult to match theoretically. Most models predict too many many-sided bubbles and mean field theories many too many. The Potts does best, but still has too many many-sided bubbles and hence excessively large moments.

If we try to match the froth to other experimental coarsening patterns the only experiment that provides a reasonable match is Fradkov *et al.*'s measurement in Al foil (23). The side distributions are similar in shape. The chief difference is the prominence of the tail in the metallic grain growth. The Potts model also is within range of the results for the foil for all values, though consistently on the low side for the moments.

The apparent failure of topological mean field theories and network models to predict the moments in the soap froth correctly, shows that there is an anti-many-sided bubble bias built into the soap froth (5, 7). Marder's mean field theory, which assumes a positive correlation, is further from the experiment than mean field theories which assume uncorrelated redistribution (4). Any model of froth needs to include an anticorrelation in side shedding: that many-sided bubbles preferentially lose sides and few-sided bubbles preferentially gain sides. Unfortunately, since the experimentally observed angle deviations could contribute to an anticorrelation, we cannot conclude that anticorrelation is characteristic of "ideal" coarsening.

In the case of the Potts model and metallic grain growth the discrepancy may arise from stiffness caused by anisotropy. The excess curvature which opposes increases in number of sides for many-sided bubbles is masked in the presence of anisotropy. In this case we would expect that the third moment of the scaling state would increase with increasing anisotropy and decrease with increasing temperature. We are currently investigating the dependence of the distribution functions on the relative orientational anisotropies of the Potts model lattice. For lower anisotropies and higher temperatures, the frequency of many-sided bubbles should decrease. An alternative mechanism is the relatively slow rate of diffusion along grain boundaries. Large, many-sided bubbles may not "know" how many sides they have. Again, careful measurements using different materials or lattices and temperatures are needed.

The time evolution of the area histograms for the two dimensional soap froth, $\rho(a/\langle a\rangle)$, is similar to that of the side distributions. At short times the distribution peaks sharply around the average area (corresponding to a pattern composed primarily of uniform sized six-sided bubbles). In time, the most probable size gradually decreases to zero while the large area tail of the distribution gradually lengthens. This broadening comes about because the fraction of shrinking small bubbles with near zero absolute area remains essentially constant, while the bubbles' relative size decreases as the total length scale increases. Eventually the distribution reaches a time invariant scaling state (Fig. 5(b)). The number of small, nearly average area bubbles is greater in the Potts model simulation than the soap

froth (i.e. the distribution is narrower), but the distributions are otherwise very close. Since the widths of the area and side distributions increase and decrease together during the initial period of disordering, it seems somewhat paradoxical that in the scaling state the Potts model simulation should have a wider side distribution and narrower area distribution than the froth.

Correlations

Of the aggregate quantities derivable from the area distribution functions, the average radius of an n-sided bubble as a function of n is the most useful. If we plot $r_n=\langle a_n^{1/2}\rangle/\langle a^{1/2}\rangle$ (Fig. 7) the graph is essentially linear, with just a hint of rollover for large n (24, 25). In this case, because of the scarcity of many-sided bubbles, we may well be observing a selection effect: large many-sided bubbles are more likely to intersect the frame boundary than small bubbles and are hence more likely to be excluded from consideration, resulting in a low apparent size for large n. The soap froth and square and triangular lattice Potts model simulations give essentially identical results. The metal foil of Fradkov *et al.* has slightly larger many-sided grains (23). The mean field theories predict excessively large few-sided bubbles (4, 6, 7). Together they provide added evidence for the existence of an anticorrelation in side redistribution in the froth, which is apparent in the uncorrelated mean field theory's predictions of larger size few-sided bubbles.

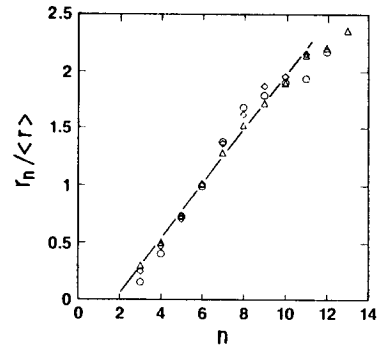

Figure 7 -- Fractional radius in the scaling state of an n-sided grain versus n for the soap froth (circles) and the square lattice (diamonds) and triangular lattice (triangles) Potts models.

The simplest side correlation function to measure is the average number of sides of the neighbors of an n-sided bubble, $m(n)$. Weaire has argued on physical grounds that:

$$m(n) = 6 - a + (6a + \mu_2)/n, \qquad (5)$$

where μ_2 is the second moment of the side distribution and a is a constant of order one (26). It is observed to hold both in the froth and the Potts model (3, 22).

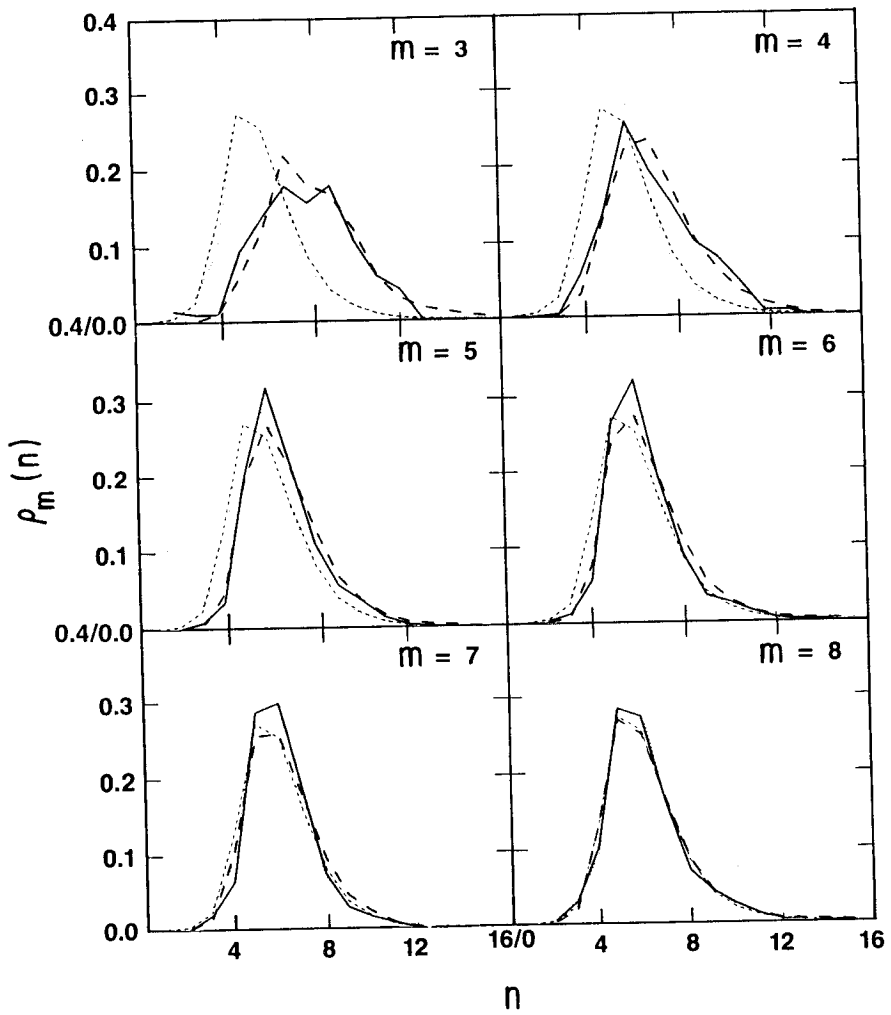

Figure 8 -- Nearest neighbor side correlations in the scaling state for soap froth (solid) and square lattice Potts model (dashed). Light dashed lines show the distribution in Fig. 5 (a).

In Fig. 8 we present $\rho_m(n)$, the probability that a bubble next to an m-sided bubble has n sides. As expected we find that few-sided bubbles tend to be near many-sided bubbles. The converse does not hold, however. Six-sided bubbles cluster together, and seven-sided bubbles attract six-sided bubbles. Even more surprising, the distribution of neighbors of eight-sided bubbles is essentially the total distribution. Discounting the bias towards many- and few-sided bubbles that we have noted in the simulation, the behavior of the distributions as a function of m is identical for the Potts model and the froth.

Conclusion

We briefly summarize our understanding of "ideal" two-dimensional coarsening. 1) We understand the process by which an initially well ordered cellular pattern reaches a scaling state. The early time behavior of the Potts model differs from that of the froth because the model's hexagonal bubbles are more stable than the froth's. We do not know whether this difference is a finite size effect due to the coarse graining of the lattice or is a fundamental difference in the way six-sided bubbles are affected by side redistribution. 2) While we do not yet understand completely the reason why many materials coarsen with an exponent less than one, changes in diffusion constants and orientational anisotropies provide reasonable mechanisms. 3) We assert the existence of a universal distribution function for two dimensional coarsening which underlies the actual observations in the soap froth, two dimensional grain growth in metals and the Potts model. However, the soap froth has a lower frequency of many-sided bubbles than the Potts model, and the Potts model than metallic grain growth and we have no way to determine whether a larger or smaller frequency of many-sided bubbles is "ideal". In each of the systems studied to date, there is some non-ideal effect (film thickening, anisotropy, disequilibrium) which provides a plausible mechanism to change the scaling state distributions. It seems probable, however, that the soap froth comes closest to ideal behavior. We need better experimental data on the scaling states and redistribution correlations in both experiment and theory to determine which of these mechanisms are significant. We can simulate two dimensional grain growth with good success, but we still do not know what the properties of "ideal" grain growth are.

References

1. H. V. Atkinson, "Theories of Normal Grain Growth in Pure Single Phase Systems," Acta. Met. , 36 (1988), 469-491.

2. J. A. Glazier, "Dynamics of Two Dimensional Patterns," (Ph.D. thesis, University of Chicago, 1989).

3. J. A. Glazier, M. P. Anderson, and G. S. Grest, "Coarsening in the two dimensional soap froth and the large Q Potts model: A detailed comparison," Philos. Mag. B , (1990), to appear.

4. M. Marder, "Soap-bubble growth," Phys. Rev. A , 36 (1987), 438-440.

5. V. E. Fradkov, D. G. Udler, and R. E. Kris, "Computer simulation of two-dimensional normal grain growth (the 'gas' approximation)," Philos. Mag. Letters , 58 (1988), 670-674.

6. V. E. Fradkov, L. S. Shvindlerman, and D. G. Udler, "Computer simulation of grain growth in two dimensions," Scripta. Met. , 19 (1985), 1285-1290. Also V. E. Fradkov and D. G. Udler, "Normal Grain Growth in 2-D Polycrystals," (Academy of Sciences of the U.S.S.R., Institute of Solid State Physics), (1989), preprint.

7. C. W. J. Beenakker, "Evolution of Two-Dimensional Soap-Film Networks," Phys. Rev. A , 37 (1988), 1697-1704.

8. H. J. Frost and C. V. Thompson, "Microstructural Evolution in thin films," in Computer Simulation of Microstructural Evolution , (Warrendale PA: The Metallurgical Society, 1986), 33-47.

9. D. Weaire and J. P. Kermode, "The evolution of the structure of a two-dimensional soap froth," Philos. Mag. B , 47 (1983), L29-L31.

10. D. Weaire and J. P. Kermode, "Computer Simulation of a two-dimensional soap froth: I. Method and motivation," Philos. Mag. B , 48 (1983), 245-259.

11. H. J. Frost, C. V. Thompson, C. L. Howe, and J. Whang, "A two-dimensional computer simulation of capillarity-driven grain growth: Preliminary results," Scripta. Met. , 22 (1988), 65-70.

12. K. Kawasaki, T. Nagai, and K. Nakashima, "Vertex Models of Two-Dimensional Grain Growth," Phil Mag. B , (1989), preprint.

13. M. P. Anderson, D. J. Srolovitz, G. S. Grest, and P. S. Sahni, "Computer simulation of grain growth-I. Kinetics," Acta. Met. , 32 (1984), 783-791.

14. D. J. Srolovitz, M. P. Anderson, P. S. Sahni, and G. S. Grest, "Computer simulation of grain growth-II. Grain size distribution, topology, and local dynamics," Acta. Met. , 32 (1984), 793-802.

15. G. S Grest, D. J. Srolovitz, and M. P. Anderson, "Domain-growth kinetics for the Q-state Potts model in two and three dimensions," Phys. Rev. B , 38 (1988), 4752-4760.

16. J. Wejchert, D. Weaire, and J. P. Kermode, "Monte Carlo simulation of the evolution of a two-dimensional soap froth," Philos. Mag. B , 53 (1986), 15-24.

17. J. A. Glazier, S. P. Gross, and J. Stavans, "Dynamics of two-dimensional soap froths," Phys. Rev. A , 36 (1987), 306-312.

18. J. von Neumann, "Discussion," in Metal Interfaces , (Cleveland, OH: American Society for Metals, 1952), 108-110.

19. Fu Tingliang, "A Study of Two-Dimensional Soap Froths" (M.S. thesis, Trinity College, Dublin, 1986).

20. J. A. Glazier and J. Stavans, "Non-Ideal Effects in the Two Dimensional Soap Froth," Phys. Rev. A , 40 (1989), 7398-7401. Also D. Weaire, "Comment on 'Soap Froth Revisited,'" (1990), preprint.

21. C. S. Smith, "Grain shapes and other metallurgical applications of topology," in Metal Interfaces , (Cleveland OH: American Society for Metals, 1952), 65-108.

22. J. Stavans and J. A. Glazier, "Soap Froth Revisited: Dynamic Scaling in the Two-Dimensional Froth," Phys. Rev. Lett. , 62 (1989), 1318-1321.

23. V. E. Fradkov, A. S. Kravchenko, and L. S. Shvindlerman, "Experimental investigation of normal grain growth in terms of area and topological class," Scipta. Met. , 19 (1985), 1291-1296.

24. F. T. Lewis, "The correlation between cell division and the shapes and sizes of prismatic cells in the epidermis of cucumis," Anatomical Record , 38 (1928), 341-362.

25. F. Feltham, "Grain Growth in Metals," Acta. Met. , 5 (1957), 97-105.

26. C. J. Lambert and D. Weaire, "Theory of the arrangement of Cells in a Network," Metallography , 14 (1981), 307-318.